



CHORUS

This is the accepted manuscript made available via CHORUS. The article has been published as:

Critical fluctuations and the rates of interstate switching near the excitation threshold of a quantum parametric oscillator

Z. R. Lin, Y. Nakamura, and M. I. Dykman

Phys. Rev. E **92**, 022105 — Published 5 August 2015

DOI: [10.1103/PhysRevE.92.022105](https://doi.org/10.1103/PhysRevE.92.022105)

Critical fluctuations and the rates of interstate switching near excitation threshold of a quantum parametric oscillator

Z. R. Lin,¹ Y. Nakamura,^{1,2} and M. I. Dykman³

¹*RIKEN Center for Emergent Matter Science (CEMS), Wako, Saitama 351-0198, Japan*

²*Research Center for Advanced Science and Technology (RCAST),
The University of Tokyo, Meguro-ku, Tokyo 153-8904, Japan*

³*Department of Physics and Astronomy, Michigan State University, East Lansing, MI 48824, USA*

We study the dynamics of a nonlinear oscillator near the critical point where period-two vibrations are first excited with the increasing amplitude of parametric driving. Above the threshold, quantum fluctuations induce transitions between the period-two states over the quasienergy barrier. We find the effective quantum activation energies for such transitions and their scaling with the difference of the driving amplitude from its critical value. We also find the scaling of the fluctuation correlation time with the quantum noise parameters in the critical region near the threshold. The results are extended to oscillators with nonlinear friction.

PACS numbers: 05.40.-a, 03.65.Yz, 05.60.Gg, 85.25.Cp

I. INTRODUCTION

Parametrically driven oscillators are of fundamental interest as a platform for studying quantum physics away from thermal equilibrium in well-characterized systems. Examples include noise squeezing, low-noise quantum amplification, photon generation, quantum measurements, and the preparation of a superposition of coherent states in a dissipative environment [1–9]. Classically, parametrically excited vibrational states are states with a broken discrete time-translation symmetry, as their period is twice the modulation period [10]. Excitation of period two vibrations with the increasing driving strength is somewhat reminiscent of the mean-field ferromagnetic phase transition with lowering temperature.

A distinctive feature of the parametric oscillator is the possibility to have a stable state with unbroken time-translation symmetry along with the stable period-two vibrational states (more precisely, such states are called asymptotically stable). In the symmetric state, vibrations are either not excited or there may be small-amplitude vibrations with the same period as the driving. In the parameter space there is a critical point where this state and the period-two states merge.

In this paper we study quantum fluctuations near the critical point. They are strong and slow. We find the long-time behavior of their correlation functions and the scaling of the correlation time with \hbar and temperature. As the system moves deeper into the range of coexisting period-two states, in the neglect of fluctuations it would localize in one of them or in the symmetric state, if it is also stable. A major manifestation of quantum fluctuations is switching between the states. We identify the switching mechanism and find the switching rates. We study how the rates scale with the driving amplitude and how there occurs a crossover to the previously explored scaling far from the critical point.

We focus on quantum effects for weakly damped oscillators, where the decay rate Γ is small compared to the

oscillator eigenfrequency ω_0 . This condition is usually met in the experiments with superconducting microcavities and with Josephson-junction based systems used in quantum information. For weakly damped oscillators, nonlinearity becomes substantial already for comparatively small vibration amplitudes, once the nonlinearity-induced shift of the vibration frequency becomes comparable with Γ . It is the nonlinearity that leads to multistability of forced vibrations. Even though the nonlinear effects are strong, they occur in the range of comparatively small vibration amplitudes, and classically, the oscillator motion is almost sinusoidal vibrations with slowly varying amplitude and phase.

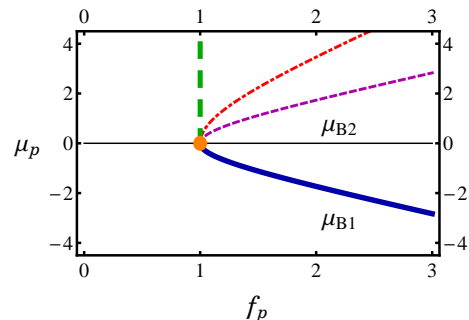


FIG. 1. The relation between the parameters of the driving field where the number of stable vibrational states changes. Parameters μ_p and f_p characterize the scaled detuning of the field frequency from resonance and the scaled field amplitude, respectively, see Eq. (5). For $f_p < 1$ or $\mu_p < \mu_{B1}$ the oscillator has no period-two vibrational states. In the region $f_p > 1$ and $\mu_p > \mu_{B1}$ there are two stable period-two states. For $\mu_p > \mu_{B2}$ the state with no period-two vibrations is stable, too. On the long-dashed line the stable and unstable period-two states coalesce. The point $\mu_p = 0$, $f_p = 1$ where the three bifurcation lines merge is the critical point. The dot-dashed line shows where the three stable states are equally occupied in the stationary regime.

Classically, the dynamics of a driven underdamped os-

illator is determined by two parameters, the scaled frequency and amplitude of the driving [10]. The analysis of the dynamics is simplified near bifurcation parameter values, where the number of the stable vibrational states changes. In this region one of the motions becomes slow, an analog of the “soft mode” [11]. The bifurcation relation between the oscillator parameters in the case of close-to-resonant parametric driving is shown in Fig. 1.

The possibility to describe the dynamics by a single dynamical variable also significantly simplifies quantum analysis [12]. Such variable commutes with itself at different times, and therefore its dynamics is essentially classical. However, the fluctuations are quantum, because the noise that causes them has quantum origin and its intensity is $\propto \hbar$ for low temperature. As we show, this picture applies near the critical point. We note that, in terms of the Floquet states of the modulated oscillator, this case corresponds to the distance between the quasienergy levels being much smaller than their width due to dissipation.

In the penultimate section of the paper we consider the dynamics near the critical point in the presence of nonlinear friction, where the friction coefficient is quadratic in the vibration amplitude. Such friction plays an important role in various types of mesoscopic vibrational systems [9, 13, 14]. The bifurcation diagram in this case differs from that in Fig. 1 and the critical point does not correspond to the minimal strength of the driving field. However, as we show, the method we develop to analyze quantum fluctuations near the critical point can be extended to this case as well.

II. THE MODEL

We consider a parametrically driven oscillator with the Duffing (Kerr) nonlinearity. The Hamiltonian of the oscillator reads

$$H_0 = \frac{1}{2}p^2 + \frac{1}{2}\omega_0^2 q^2 + \frac{1}{4}\gamma q^4 + \frac{1}{2}q^2 F \cos \omega_F t, \quad (1)$$

where q and p are the oscillator coordinate and momentum, the mass is set equal to one, and γ is the anharmonicity parameter. Parameter F gives the amplitude of the driving, whereas ω_F is the driving frequency.

We assume the driving to be resonant and not too strong,

$$|\delta\omega| \ll \omega_0, \quad \delta\omega = \frac{1}{2}\omega_F - \omega_0; \quad |\gamma|\langle q^2 \rangle \ll \omega_0^2. \quad (2)$$

It is convenient to change to the rotating frame using the standard canonical transformation $U(t) = \exp(-ia^\dagger a \omega_F t/2)$, where a^\dagger and a are the raising and lowering operators of the oscillator. We introduce slowly varying in time dimensionless coordinate Q and momentum P , using as a scaling factor the characteristic amplitude of forced vibrations $C_p = |2F_c/3\gamma|^{1/2}$ [parameter

F_c is defined below in Eq. (7)],

$$\begin{aligned} U^\dagger(t)qU(t) &= C_p(Q \cos \varphi + P \sin \varphi), \\ U^\dagger(t)pU(t) &= -\frac{1}{2}C_p\omega_F(Q \sin \varphi - P \cos \varphi) \end{aligned} \quad (3)$$

with $\varphi = \frac{1}{2}\omega_F t + \frac{1}{4}\pi$. The commutation relation between P and Q is

$$[P, Q] = -i\lambda_p, \quad \lambda_p = 3|\gamma|\hbar/(\omega_F F_c). \quad (4)$$

Parameter $\lambda_p \propto \hbar$ plays the role of the Planck constant in the quantum dynamics in the rotating frame. This is the small parameter of the theory, $\lambda_p \ll 1$. Note that it is determined by the oscillator nonlinearity, $\lambda_p \propto \gamma$. As we will see, for $\lambda_p \ll 1$ the oscillator dynamics near the critical point is semiclassical.

For characteristic $|Q|, |P| \lesssim 1$, where $\langle q^2 \rangle \lesssim C_p^2$, the last inequality in Eq. (2) implies $F \ll \omega_0^2$. To simplify the analysis near the critical point, in Eqs. (3) and (4) we choose the variables in the form that slightly differs from that in Ref. 12.

In the range (2) the oscillator dynamics can be analyzed in the rotating wave approximation (RWA). The Hamiltonian in the rotating frame is $U^\dagger H_0 U - i\hbar U^\dagger \dot{U} = (F_c^2/6\gamma)\hat{g}_p$. Operator $\hat{g}_p = g_p(Q, P)$ is independent of time and has the form

$$\begin{aligned} g_p(Q, P) &= \frac{1}{4}(P^2 + Q^2)^2 - \frac{1}{2}\mu_p(P^2 + Q^2) \\ &\quad + \frac{1}{2}f_p \text{sgn}\gamma(QP + PQ), \\ \mu_p &= \frac{\omega_F(\omega_F - 2\omega_0)}{F_c} \text{sgn}\gamma, \quad f_p = F/F_c. \end{aligned} \quad (5)$$

The eigenvalues of \hat{g}_p (multiplied by $F_c^2/6\gamma$) give the oscillator quasienergies.

In Eq. (5), parameter f_p is the scaled driving amplitude F ; in what follows we assume $f_p > 0$. Parameter μ_p gives the detuning of the driving frequency from twice the oscillator eigenfrequency. The scaling factor in both f_p and μ_p is the critical amplitude F_c needed for parametric excitation of the oscillator.

Relaxation of the oscillator results from the coupling to a thermal bath. The coupling leads to oscillator decay due to scattering by the bath excitations. For a weak coupling, one of the most important scattering mechanisms is scattering with energy transfer $\approx \hbar\omega_0$ in an elementary event [15–17]. It comes from the coupling, which is linear in the oscillator coordinate and/or momentum. In a phenomenological description of the oscillator dynamics such scattering corresponds to a friction force $-2\Gamma\dot{q}$. The friction coefficient Γ is simply expressed in terms of the appropriate correlator of the thermal bath variables.

It is important for what follows that relaxation comes along with a quantum noise. The equations of motion for slow variables Q, P in the rotating frame in dimensionless time $\tau = \Gamma t$ read

$$\begin{aligned} \dot{Q} &= -i\lambda_p^{-1}[Q, \hat{g}_p] \text{sgn}\gamma - Q + \hat{f}_Q(\tau), \\ \dot{P} &= -i\lambda_p^{-1}[P, \hat{g}_p] \text{sgn}\gamma - P + \hat{f}_P(\tau). \end{aligned} \quad (6)$$

Here, $\dot{A} \equiv dA/d\tau$. We have set

$$F_c = 2\Gamma\omega_F, \quad (7)$$

in which case, indeed, F_c is the threshold value of the driving amplitude, as will be seen below.

In Eq. (6), $\hat{f}_{Q,P}$ are quantum noise operators. The noise is δ -correlated in slow time, cf. [12],

$$\begin{aligned} \langle \hat{f}_Q(\tau)\hat{f}_Q(\tau') \rangle_b &= \langle \hat{f}_P(\tau)\hat{f}_P(\tau') \rangle_b = 2\mathcal{D}\delta(\tau - \tau'), \\ \langle [\hat{f}_Q(\tau), \hat{f}_P(\tau')] \rangle_b &= 2i\lambda_p\delta(\tau - \tau'), \\ \mathcal{D} &= \lambda_p(\bar{n} + 1/2), \quad \bar{n} = [\exp(\hbar\omega_0/k_B T) - 1]^{-1}. \end{aligned} \quad (8)$$

Here, \bar{n} is the oscillator Planck number and $\langle \cdot \rangle_b$ means averaging over the bath state. Parameter \mathcal{D} plays the role of the effective temperature of the quantum noise, $\mathcal{D} \propto \lambda_p \propto \hbar$ for $\hbar\omega_0 \gg k_B T$. We assume that temperature is not too high, so that $\mathcal{D} \ll 1$. The commutation relation in Eq. (8) guarantees that the commutator $[Q, P] = i\lambda_p$ does not change in time. The noise correlators are understood in the Stratonovich sense [18]; in particular, $\langle [\hat{f}_Q(\tau), P(\tau)] \rangle_b = \langle [Q(\tau), \hat{f}_P(\tau)] \rangle_b = i\lambda_p$.

III. SLOW QUANTUM DYNAMICS NEAR THE CRITICAL POINT

The stable vibrational states of the oscillator are given by the stable stationary solutions of Eq. (6) without noise. The bifurcation values of the parameters f_p, μ_p , where the number of the stable states changes, lie on the lines $\mu_p = \pm\mu_B(f_p)$ and $(\mu_p \geq 0, f_p = 1)$ on the (f_p, μ_p) -plane,

$$\mu_B = (f_p^2 - 1)^{1/2}. \quad (9)$$

The bifurcation lines are shown in Fig. 1. For $\mu_p < \mu_{B1} \equiv -\mu_B$ and for $f_p < 1$ the only stable state of the oscillator is $Q = P = 0$. The amplitude of period-two vibrations in this state is zero, and below we call it the zero-amplitude state. At $\mu_p = \mu_{B1}$ this state becomes unstable. For larger μ_p or f_p the oscillator has two stable states, which correspond to period-two vibrations in the lab frame with the reduced squared amplitude $Q^2 + P^2 = \mu_p + (f_p^2 - 1)^{1/2}$ and with the phases differing by π . For $\mu_p = \mu_{B2}$ the state $Q = P = 0$ becomes stable and there emerge two unstable states, which correspond to unstable period-two vibrational states in the lab frame[10]. The values of the control parameter μ_{B1} and μ_{B2} correspond to the supercritical and subcritical pitchfork bifurcations [11]. On the line $f_p = 1, \mu_p > 0$ the stable and unstable states, which correspond to period-two vibrations, coalesce.

At the critical point $(\mu_p = 0, f_p = 1)$ all three bifurcation lines merge. Such merging is robust, it does not disappear if the model is slightly changed, although the position of the critical point can change. The associated strong singularity of the dynamics in the absence of noise leads to comparatively strong fluctuation effects.

Near the critical point, for small Q, P the coordinate Q varies in time much slower than P . This is seen from the linearized equations (6), which in the absence of noise take the form $\dot{Q} = (f_p - 1)Q - \mu_p P \text{sgn}\gamma, \dot{P} = -(f_p + 1)P + \mu_p Q \text{sgn}\gamma$.

Because $Q(\tau)$ is slow, $P(\tau)$ adiabatically follows $Q(\tau)$. For the dimensionless time $\tau \gg 1$, function $P(\tau)$ can be expressed in terms of $Q(\tau)$ by disregarding the quantum noise $\hat{f}_P(\tau)$ and setting $\dot{P} = 0$. The latter equation gives a function $P_{\text{ad}}(Q(\tau))$. Substituting $P = P_{\text{ad}}(Q)$ into the full nonlinear equation for \dot{Q} , one obtains

$$\dot{Q} \approx -\partial_Q U(Q) + \hat{f}_Q(\tau), \quad (10)$$

$$U(Q) = \frac{1}{4}Q^2 [\mu_p^2 - (f_p^2 - 1)] + \frac{1}{4}Q^4 \left(-\mu_p + \frac{1}{3}Q^2 \right)$$

$[U(Q)$ has an extra factor $2/(f_p + 1)$ which is set equal to 1, to the leading order in $f_p - 1$]. To justify disregarding $\hat{f}_P(\tau)$, we note that fluctuations of $P(\tau)$ due to $\hat{f}_P(\tau)$ are small, $\langle [P(\tau) - P_{\text{ad}}(Q(\tau))]^2 \rangle \approx \mathcal{D}/(f_p + 1)$. Since the linear in $P(\tau)$ term in the full equation for \dot{Q} is proportional to the small parameter μ_p , the effect on $Q(\tau)$ from these fluctuations is small compared to that from the noise $\hat{f}_Q(\tau)$. For times $\tau \gg 1$, the distribution over P is Gaussian, $\propto \exp\{-[P - P_{\text{ad}}(Q)]^2/2\mathcal{D}(f_p + 1)\}$, it is squeezed around $P_{\text{ad}}(Q)$.

A. The effective potential for the slow variable

For $\mu_{B1} < \mu_p < \mu_{B2}$, the effective potential $U(Q)$, Eq. (10), has a local maximum at $Q = 0$ and two symmetric minima at $Q_{1,2} = \pm(\mu_B + \mu_p)^{1/2}$. The minima correspond to the stable period-two vibrations in the lab frame.

For $\mu_p > \mu_{B2}, f_p^2 > 1$, function $U(Q)$ still have the minima at $Q_{1,2}$, but now it has a local minimum at $Q = 0$ and two additional local maxima at $Q = \pm(\mu_p - \mu_B)^{1/2}$. The minimum at $Q = 0$ corresponds to the stable zero-amplitude state. The local maxima correspond to unstable period-two vibrations.

The behavior of the oscillator near the onset of period-two vibrations at μ_{B1} has similarities with the mean-field picture of the critical behavior at the second-order phase transition. The time-translation symmetry of the stable stationary state at $Q = 0$ is spontaneously broken and there emerge two vibrational states with equal amplitudes and opposite phases and with period $4\pi/\omega_F$. Such behavior is usually described by an effective potential which is quartic in the coordinate Q .

A key observation is that, near the critical point $f_p = 1, \mu_p = 0$, it is necessary to keep the sixth-order term in $U(Q)$. This follows from Eq. (10). The system becomes softer than at the bifurcation point far away from the critical point. Such form of the potential reminds the Landau free energy for a system that can undergo a

first-order phase transition, and indeed, an analog of this transition can occur in the driven oscillator, see below.

B. The quantum Fokker-Planck equation

Equation (10) has the form of the Langevin equation of a classical particle with one dynamical variable (half-degree of freedom) driven by a δ -correlated noise. Indeed, $\hat{f}_Q(\tau)$ and $Q(\tau)$ commute, and therefore $[Q(\tau), Q(\tau')] = 0$. However, the noise has quantum origin, its correlator (8) explicitly contains \hbar . The slow quantum fluctuations can be alternatively described by the Fokker-Planck equation for the probability density $\rho(Q, \tau)$. From Eq. (10), it reads

$$\partial_\tau \rho = \partial_Q(\rho \partial_Q U) + \mathcal{D} \partial_Q^2 \rho. \quad (11)$$

The stationary distribution of the oscillator near the critical point has the Boltzmann form

$$\rho_{\text{st}}(Q) = Z^{-1} \exp[-U(Q)/\mathcal{D}], \quad (12)$$

where $Z = \int dQ \exp[-U(Q)/\mathcal{D}]$ is the effective partition function. The evolution of this distribution with varying f_p is shown in Fig. 2.

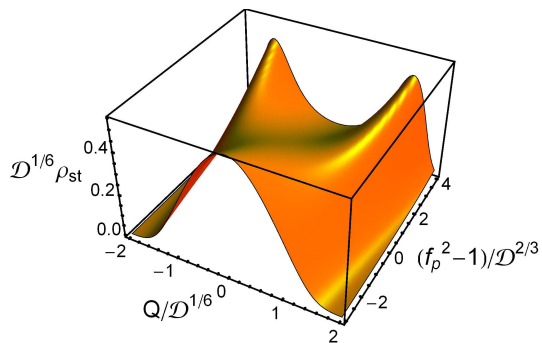


FIG. 2. Evolution of the stationary distribution $\rho_{\text{st}}(Q)$ with varying amplitude of the driving field for $\mu_p = 0$. For $f_p^2 < 1$ the distribution has a single broad maximum at $Q = 0$. With increasing f_p there are developed two sharp maxima at the positions that correspond to the period-two vibrational states.

The full stationary Wigner distribution is a product of $\rho_{\text{st}}(Q)$ and a Gaussian distribution over P , with the position of the maximum over P being Q -dependent. Function $\rho_{\text{st}}(Q)$ can be thought of as the integral over P of this full distribution. The distribution (12) is maximal at the minima of $U(Q)$, i.e., at the values of Q that correspond either to the stable states of the oscillator. Near the critical point the distribution is broad, which corresponds to large fluctuations in this range.

IV. SCALING OF THE RATES OF QUANTUM-FLUCTUATION INDUCED SWITCHING

Once the depth of the minima of $U(Q)$ becomes large compared to $\lambda_p(2\bar{n} + 1)$, the dynamics of the oscillator is characterized by two very different time scales. One is the relaxation time $1/U''(Q)$ for Q near the stable states. The other is a much slower time over which the oscillator can switch between the minima due to comparatively rare large fluctuations. The switching rate W_{sw} is given by the Kramers theory [19] of thermally activated switching over a potential barrier. This theory immediately extends in the present case to quantum fluctuations, even though there is, of course, no thermal activation for low temperatures. In dimensionless time $\tau = \Gamma t$

$$\begin{aligned} W_{\text{sw}} &= \Omega_{\text{sw}} \exp(-R_A/\lambda_p), & R_A &= \Delta U/(\bar{n} + 1/2), \\ \Omega_{\text{sw}} &= [|U''(Q_S)|U''(Q_a)]^{1/2}/2\pi, \\ \Delta U &= U(Q_S) - U(Q_a). \end{aligned} \quad (13)$$

Here, Q_a is the position of the stable state (attractor) from which the oscillator switches and Q_S is the position of the adjacent local potential maximum [a saddle point on the (Q, P) -plane] over which the switching occurs. Function R_A is the quantum activation energy for the switching, it is proportional to the height of the potential barrier overcome in the switching.

Remarkably, Eq. (13) for the switching rate has the same structure as the expression for the rate of tunneling from a potential well of $U(Q)$ in the sense that the rate is exponential in $1/\lambda_p \propto 1/\hbar$. However, switching occurs not via tunneling under the barrier of $U(Q)$ but by going over the barrier. Tunneling requires the fast variable P to be involved. Therefore the tunneling exponent is parametrically larger than R_A and the tunneling rate is exponentially smaller [20].

The states between which the switching occurs and the rate W_{sw} depend on the parameter region on the bifurcation diagram in Fig. 1. We start with the region $\mu_{B1}(f_p) < \mu_p < \mu_{B2}(f_p)$. Here, the oscillator is bistable. It can switch from one period-two state to the other. By symmetry, the switching rates for the both states are the same. In Eq. (13) $Q_a = \pm(\mu_B + \mu_p)^{1/2}$, depending on the initially occupied state. The switching occurs over the unstable state $Q_S = 0$.

The dependence of the activation energy R_A for switching between the period-two states on the parameters is shown in Fig. 3. For exact resonance, $\mu_p = 0$, it follows from Eq. (10) that $R_A = (f_p^2 - 1)^{3/2}/3(2\bar{n} + 1)$. In this case R_A displays a power law dependence on the distance from the critical field amplitude $f_p - 1$. The scaling exponent is $3/2$. For nonzero μ_p , the behavior becomes more complicated and is not described by a simple power law. Close to the bifurcation line $\mu_{B1}(f_p)$, function R_A scales as a power of the distance from $\mu_{B1}(f_p)$, $R_A \approx \mu_B(\mu_p - \mu_{B1})^2/2(2\bar{n} + 1)$, cf. Ref. 12. We note that the scaling of the switching rates near a bifurcation

point of a different type has been observed for resonantly driven Josephson junction based quantum oscillators [21].

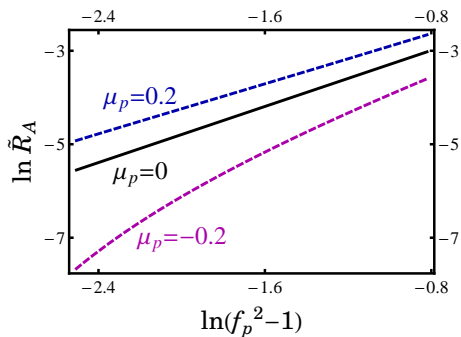


FIG. 3. The quantum activation energy $\tilde{R}_A = (\bar{n} + 1/2)R_A$ for switching between the parametrically excited period-two vibrational states with opposite phases. In the shown range of the scaled driving field amplitude $1.04 < f_p \equiv F/F_c < 1.2$ and the scaled frequency detuning $|\mu_p| < \mu_B(f_p)$, the period-two vibrations are the only stable states of the oscillator.

A different situation occurs in the range $\mu_p > \mu_B(f_p)$ and $f_p > 1$. Here, far from the bifurcation lines in Fig. 1 the potential $U(Q)$ has three local minima separated by two local maxima. Interstate switching occurs via a transition from a minimum of $U(Q)$ over the adjacent maximum. This means that from the stable period-two states the oscillator can switch to the zero-amplitude state and vice versa, but direct switching between the period-two states is exponentially unlikely.

The switching activation energies in the region of tristability are shown in Fig. 4; R_{A1} and R_{A0} refer to switching from a period-two state to the zero-amplitude state and from the zero-amplitude state to one of the period-two states, respectively. To find R_{A1} , one sets in Eq. (13) $Q_a = \pm(\mu_p + \mu_B)^{1/2}$, whereas to find R_{A0} one sets $Q_a = 0$; in the both cases, $Q_S = \pm(\mu_p - \mu_B)^{1/2}$. Interestingly, from Eq. (10), the activation energy R_{A1} displays simple scaling behavior, $R_{A1} = (f_p^2 - 1)^{3/2}/3(\bar{n} + 1/2)$ independent of μ_p . The activation energy of switching from the zero-amplitude state displays a more complicated behavior. It decreases with the increasing field amplitude. Near the bifurcation line $\mu_p = \mu_B(f_p)$ we have $R_{A0} \approx \mu_B(\mu_p - \mu_B)^2/2(2\bar{n} + 1)$, in agreement with the previous work [12].

In the stationary regime, for $R_{A1} > R_{A0}$ it is exponentially more probable for the system to be in the state of period-two vibrations. On the other hand, for $R_{A0} > R_{A1}$, preferentially occupied is the zero-amplitude state, where the period-two vibrations are not excited. The interrelation between the field amplitude and frequency where $R_{A1} = R_{A0}$ corresponds to an analog of a first-order phase transition: here the populations of the different stable states of the oscillator are close to each other. From Eq. (10), near the critical point the “phase-transition” value of f_p is given by expression $(f_p^2 - 1)^{1/2} = \mu_p/2$. It is shown by the dot-dashed line

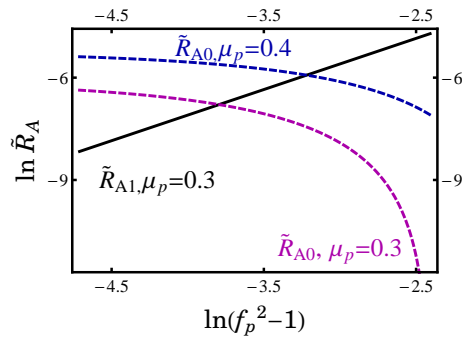


FIG. 4. The quantum activation energies $\tilde{R}_{A1} = (\bar{n} + 1/2)R_{A1}$ and $\tilde{R}_{A0} = (\bar{n} + 1/2)R_{A0}$ for switching from a state of period-two vibrations to the zero-amplitude state and from the zero-amplitude state to one of the states of period-two vibrations, respectively. The curves refer to the region of tristability, where the scaled driving field amplitude $f_p > 1$ and the scaled frequency detuning $\mu_p > \mu_B(f_p)$.

in Fig. 1.

V. QUANTUM FLUCTUATIONS IN THE IMMEDIATE VICINITY OF THE CRITICAL POINT

Close to the critical point, where $|f_p^2 - 1| \lesssim \mathcal{D}^{2/3}$, $|\mu_p| \lesssim \mathcal{D}^{1/3}$, the stationary distribution (12) is almost flat, as seen from Fig. 2. This indicates anomalously large quantum fluctuations of the oscillator variable Q (whereas the fluctuations of the other variable, P , are squeezed). The fluctuational mean-square displacement is $\langle Q^2 \rangle \sim \mathcal{D}^{1/3}$, whereas far from the critical region the mean-square displacement about a stable state is $\sim \mathcal{D}$ ($\mathcal{D} \propto \hbar$ is the small parameter of the theory, $\mathcal{D} \ll 1$). In the critical region the exponents R_A/λ_p are no longer large and the concept of switching rates becomes ill-defined. One cannot separate switching from other fluctuations.

A convenient characteristic of the fluctuation dynamics is the long-time decay of the correlation functions of the oscillator. This decay is characterized by the lowest nonzero eigenvalue ν_1 of the Fokker-Planck equation (11). It can be found in a standard way [18] by reducing Eq. (11) to a Schrödinger-type equation for $\tilde{\rho}(Q) = \exp[U(Q)/2\mathcal{D}]\rho(Q)$. The quantum noise intensity \mathcal{D} can be scaled out of this equation by changing to the scaled time $\mathcal{D}^{2/3}\tau$, scaled coordinate $\mathcal{D}^{-1/6}Q$, and scaled parameters $\mathcal{D}^{-1/3}\mu_p$ and $\mathcal{D}^{-2/3}(f_p^2 - 1)$.

The dependence of the decrement ν_1 on the frequency detuning parameter $\mu_p \propto (\omega_F - 2\omega_0)/F_c$ for several values of the scaled driving field amplitude $f_p = F/F_c$ is shown in Fig. 5. It is seen that, for a given μ_p , the dynamics is slowed down, i.e., ν_1 decreases with the increasing driving amplitude. This is to be expected and is in agreement with Fig. 2. For $f_p^2 < 1$ or $(f_p^2 - 1)^{1/2} + \mu_p < 0$, the oscillator has one stable state, $Q = 0$. As f_p^2 increases, the minimum of $U(Q)$ at $Q = 0$ becomes more and more

shallow and the relaxation rate, which is related to the curvature of $U(Q)$, goes down. As f_p^2 further increases, the system goes into the regime of coexisting period-two states (via the range of coexisting three stable states, for $\mu_p > 0$, cf. Fig. 1). For large $(f_p^2 - 1)/\mathcal{D}^{2/3}$, ν_1 is determined by the exponentially small rate of interstate switching that rapidly decreases with increasing f_p , see Figs. 3 and 4.

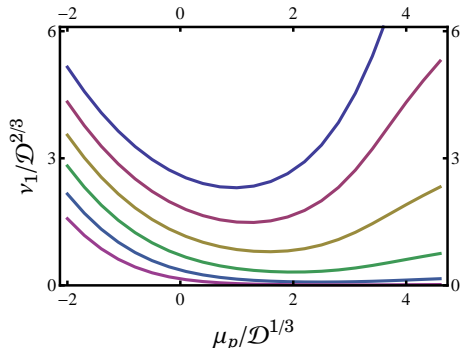


FIG. 5. The smallest nonzero eigenvalue ν_1 of the kinetic equation (11), which determines the long-time decay of the correlation functions very close to the critical point $\mu_p = 0, f_p = 1$. The curves from top down correspond to $(f_p^2 - 1)/\mathcal{D}^{2/3} = -4, -2, 0, 2, 4, 6$.

The dependence of ν_1 on the frequency detuning in Fig. 5 is profoundly nonmonotonic. For $f_p^2 - 1 < 0$, where the system has only one stable state, $Q = 0$, this behavior is a consequence of the nonmonotonic dependence of the curvature of $U''(0)$ on μ_p , see Eq. (10). Close to the critical point the nonparabolicity of $U(Q)$ is substantial. This is also seen from Fig. 2, which shows that the stationary probability distribution becomes profoundly non-Gaussian near the critical point. Therefore ν_1 is different from $U''(0)$. The minimum of ν_1 is reached for $\mu_p > 0$.

In the range $\mu_p > \mu_{B1} = -(f_p^2 - 1)^{1/2}$ the oscillator has two or three stable states in the neglect of fluctuations. For large $(\mu_p - \mu_{B1})/\mathcal{D}^{1/3}$, the decrement ν_1 is determined by the rate of interstate switching. This explains the decrease of ν_1 with increasing μ_p in Fig. 5 for $f_p^2 > 1$ and for not too large $\mu_p/\mathcal{D}^{1/3}$.

To understand the behavior of ν_1 for larger μ_p in the range of tristability of the oscillator, we consider the balance equations for the populations of the two period-two states $w_{1,2}$ and the zero-amplitude state w_0 ,

$$\begin{aligned} \dot{w}_0 &= -2W_{01}w_0 + W_{10}(w_1 + w_2), \\ \dot{w}_i &= W_{01}w_0 - W_{10}w_i \quad (i = 1, 2), \end{aligned} \quad (14)$$

where $W_{01} = W_{02} \propto \exp(-R_{A0}/\lambda_p)$ is the rate of switching from the zero-amplitude state to one of the period-two states and $W_{10} = W_{20} \propto \exp(-R_{A1}/\lambda_p)$ is the rate of switching from a period-two state to the zero-amplitude state.

From Eq. (14), $\nu_1 = W_{10}$ in the region of tristability where the slow dynamics is determined by inter-state

switching. The exponent R_{A1}/λ_p in Eq. (13) for the rate W_{10} is independent of μ_p , cf. Fig. 4. However, the prefactor $\Omega_{\text{sw}} \propto (f_p^2 - 1)^{1/2}[\mu_p^2 - (f_p^2 - 1)]^{1/2}$ is increasing with increasing μ_p . Therefore, somewhat unexpectedly, ν_1 starts slowly increasing with μ_p in the tristability region.

VI. EFFECT OF NONLINEAR FRICTION

Mesoscopic vibrational systems often display nonlinear friction, as mentioned in the Introduction. Phenomenologically, it is described by a friction force proportional to $-q^2\dot{q}$ or $-\dot{q}^3$; both forms lead to the same time evolution of the amplitude and phase of a weakly damped oscillator on the time scale large compared to the vibration period. A simple microscopic model that gives such a force is the quadratic in q coupling to a thermal bath [22]. The underlying elementary process is emission or absorption of bath excitations in a transition between next to nearest oscillator energy levels, with the energy transfer $\approx 2\hbar\omega_0$.

Starting with the full Hamiltonian of the oscillator coupled to a bath, one can show that, with account taken of the processes leading to nonlinear friction, the right-hand sides of the quantum Langevin equations for \hat{Q} and \hat{P} , Eqs. (6), acquire extra terms r_Q and r_P , respectively,

$$\begin{aligned} r_Q &= -\frac{1}{2}\Gamma_{\text{nl}}\{Q, Q^2 + P^2\}_+ + 2\lambda_p\Gamma_{\text{nl}}Q(2\bar{n}_2 + 1) + \hat{f}_Q^{\text{nl}}(\tau), \\ r_P &= -\frac{1}{2}\Gamma_{\text{nl}}\{P, Q^2 + P^2\}_+ + 2\lambda_p\Gamma_{\text{nl}}P(2\bar{n}_2 + 1) + \hat{f}_P^{\text{nl}}(\tau), \\ \bar{n}_2 &\equiv \bar{n}(2\omega_0) = \bar{n}^2/(2\bar{n} + 1). \end{aligned} \quad (15)$$

Here, $\{A, B\}_+ = AB + BA$. The scaled nonlinear friction coefficient Γ_{nl} is related to the phenomenological coefficient of nonlinear friction as $\Gamma_{\text{nl}} = (4\omega_0^2/3|\gamma|)\Gamma^{(2)}$, if the phenomenological friction force is written as $-8\Gamma^{(2)}\omega_0q^2\dot{q}$. The coupling to a bath that leads to nonlinear friction also leads to a renormalization of the parameter γ of conservative nonlinearity, which we assume to have been done. Interestingly, the strength of the nonlinear friction is determined by the relation between the phenomenological friction parameter $\Gamma^{(2)}$ and γ .

The quantum noise terms in Eq. (15) have the form

$$\begin{aligned} \hat{f}_Q^{\text{nl}}(\tau) &= Q(\tau_{<})\hat{f}_1^{\text{nl}}(\tau) + P(\tau_{<})\hat{f}_2^{\text{nl}}(\tau), \\ \hat{f}_P^{\text{nl}}(\tau) &= Q(\tau_{<})\hat{f}_2^{\text{nl}}(\tau) - P(\tau_{<})\hat{f}_1^{\text{nl}}(\tau), \end{aligned} \quad (16)$$

where $\tau_{<}$ indicates that the operator has to be evaluated at slow time $\tau - \epsilon$ with $\epsilon \rightarrow +0$. Functions $\hat{f}_{1,2}^{\text{nl}}(\tau)$ have zero mean and are δ -correlated in slow time, $\langle \hat{f}_1^{\text{nl}}(\tau)\hat{f}_1^{\text{nl}}(\tau') \rangle = \langle \hat{f}_2^{\text{nl}}(\tau)\hat{f}_2^{\text{nl}}(\tau') \rangle = 2\lambda_p\Gamma_{\text{nl}}(2\bar{n}_2 + 1)\delta(\tau - \tau')$, whereas $\langle [\hat{f}_1^{\text{nl}}(\tau), \hat{f}_2^{\text{nl}}(\tau')] \rangle = 4i\lambda_p\Gamma_{\text{nl}}\delta(\tau - \tau')$.

Equations (6) and (15) provide an example of quantum Langevin equations with multiplicative noise: the noise $\hat{f}_{Q,P}^{\text{nl}}(t)$ depends on the dynamical variables of the system. The time ordering in Eq. (16) shows how to calculate averages with such a noise.

A. Bifurcation diagram and the critical point

In the presence of nonlinear friction, the bifurcation diagram of the oscillator in the semiclassical limit $\lambda_p \ll 1$ changes. It can be obtained using Eqs. (6) and (15) and is shown in Fig. 6. It is instructive to compare this figure with Fig. 1 that refers to the case where there is no nonlinear friction. As in that case, stable period-two vibrations exist in the interior of the region bounded by the solid line and the long-dashed line. On the other side of the solid line the zero amplitude state is stable and there are no period-two stationary states. The relation between μ_p and f_p on the solid line is $\mu_p = \mu_{B1} = \pm(f_p^2 - 1)^{1/2}$. The line terminates at $\mu_{B1} = \Gamma_{nl}$, see below.

The equation for the long-dashed line reads

$$f_p = (\Gamma_{nl}^2 + 1)^{-1/2}(\mu_p \Gamma_{nl} + 1), \quad \mu_p \geq \Gamma_{nl}. \quad (17)$$

In the region between the long-dashed line (17) and the dashed line $\mu_{B2} = (f_p^2 - 1)^{1/2}$, $\mu_{B2} \geq \Gamma_{nl}$, the oscillator has three stable states: two period-two states and the zero-amplitude state. It also has two unstable period-two states, which merge with stable period-two states on the line (17). In the region bounded by the lines μ_{B1} and μ_{B2} period-two states are the only stable states of the oscillator. On the whole, one can picture the effect of nonlinear friction on the bifurcation diagram as if the vertical line in Fig. 1 was tilted and shifted along the line $\mu_{B2}(f_p)$.

The point

$$\mu_{p0} = (f_{p0}^2 - 1)^{1/2} = \Gamma_{nl} \quad (18)$$

is the critical point. This point is common for all three bifurcation lines. One therefore expects to see in the vicinity of this point a critical behavior similar to the one in the absence of nonlinear friction.

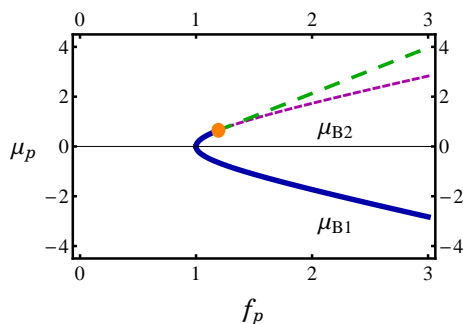


FIG. 6. The relation between the parameters of the driving field where the number of stable vibrational states changes in the presence of nonlinear friction. On the solid line μ_{B1} the stable period-two states merge with the zero-amplitude state. On the long-dashed line, Eq. (17), stable and unstable period-two states merge together. On the dashed line μ_{B2} the zero-amplitude state merges with the unstable period-two states. The dashed and long-dashed lines touch at the critical point, Eq. (18).

The analysis of fluctuations near the critical point is reminiscent of that for $\Gamma_{nl} = 0$. One can single out a slow variable Q_{nl} , which is a linear combination of Q and P . The noise $f_{Q,P}^{nl}$ associated with the nonlinear friction can be disregarded, to the leading order in λ_p . Indeed, its amplitude contains extra small factors proportional to Q, P compared to the noise associated with the linear friction. After some algebra, one then obtains for the slow variable a quantum Langevin equation for an overdamped particle of the form of Eq. (10) with Q replaced by Q_{nl} and with the potential U_{nl} of the form

$$U_{nl}(Q_{nl}) = \frac{1}{2}A_2Q_{nl}^2 + \frac{1}{4}A_4Q_{nl}^4 + \frac{1}{6}A_6Q_{nl}^6, \\ A_2 = \frac{\delta\mu_p^2}{2f_{p0}^2} - f_{p0}\delta f_p, \quad A_4 = -f_{p0}^2\delta\mu_p, \quad A_6 = \frac{1}{2}f_{p0}^6, \\ \delta\mu_p = \mu_p - \mu_{p0}, \quad \delta f_p = f_p - f_{p0} - \mu_{p0}\delta\mu_p/f_{p0}. \quad (19)$$

As in the case of linear friction, the dynamics of the system is profoundly asymmetric with respect to deviations from the critical values along the μ_p - and f_p -axes. The coefficient A_2 is quadratic in $\delta\mu_p$ but linear in δf_p , and A_4 is linear in $\delta\mu_p$ and independent of δf_p . The fluctuational range of $\delta\mu_p$, which has width $\mathcal{D}^{1/3}$, largely exceeds the fluctuational range of δf_p , which has width $\mathcal{D}^{2/3}$. We note that δf_p is counted off from the value of the scaled driving amplitude f_p calculated for a given $\delta\mu_p$ along the bifurcation line (17). In fact, this is also the case where there is no nonlinear friction, cf. Eq. (10): there f_p is independent of μ_p on the analogous line, which is given by equation $f_p = 1$. The first-order phase-transition line is given by the expression $\delta\mu_p = 2(2f_{p0}^3\delta f_p)^{1/2}$. Overall, the region of coexistence of three stable states is squeezed by nonlinear friction.

VII. CONCLUSIONS

The results of this paper refer to quantum fluctuations near the critical point of a parametric nonlinear oscillator. At this point, there merge 5 stationary vibrational states: two stable and two unstable period-two states and the zero-amplitude state. In the absence of nonlinear friction, the critical point lies at the threshold of parametric excitation, in terms of the amplitude F of the driving field. The threshold corresponds to the field frequency ω_F equal to twice the oscillator eigenfrequency ω_0 . The threshold value of the field amplitude F_c is proportional to the rate Γ of linear decay of the oscillator. In the presence of nonlinear friction, the critical point lies away from exact resonance, and the driving amplitude is $F > F_c$, see Eq. (18).

Near the critical point, the oscillator dynamics is mapped onto the dynamics of an overdamped Brownian particle. This particle is driven by quantum noise and is confined in a symmetric potential well of the sixth order in the particle displacement. The condition that the quantum noise is weak means that the dimensionless

Planck constant $\lambda_p \propto \hbar$ is small, $\lambda_p \ll 1$. In the critical region, the mean occupation number of the oscillator is large; in other words, if one thinks of the oscillator as a radiation mode of a cavity, the mean number of photons in the cavity at frequency $\omega_F/2$ is large. For $\bar{n} = 0$ (no thermal photons), at the critical point this number is $\langle a^\dagger a \rangle \approx 0.29\lambda_p^{-2/3} \gg 1$, where a^\dagger and a are the oscillator ladder operators (the photon creation and annihilation operators). The critical quantum fluctuations are profoundly non-Gaussian. The Wigner distribution is stretched along one of the quadratures, so that $\langle a^2 + a^{\dagger 2} \rangle \approx 2\langle a^\dagger a \rangle$. For finite temperatures, one should replace λ_p in the above expression with $\lambda_p(2\bar{n} + 1)$.

Critical quantum fluctuations are not only anomalously large, but also slow. In the immediate vicinity of the critical point the correlation time of the fluctuations scales as $[\hbar(2\bar{n} + 1)]^{-2/3}$. We have found the dependence of the correlation time on the frequency detuning $\omega_F - 2\omega_0$ and the amplitude F of the driving field. Unexpectedly, the dependence on the frequency detuning turned out to be nonmonotonic.

The parameter range where anomalously large fluctuations occur scales as $[\hbar(2\bar{n} + 1)]^{1/3}$ along the field frequency axis and as $[\hbar(2\bar{n} + 1)]^{2/3}$ along the field-amplitude axis. Outside this range and in the region of bi- or tri-stability, the distance between the coexisting stable states of the oscillator in phase space significantly exceeds the mean-square-root fluctuations about the states. Quantum fluctuations lead to switching between the states, but fluctuations required for the switching are comparatively large and thus rare. The switching mechanism is quantum activation. In switching the oscillator goes over an effective quasienergy barrier rather than tunneling beneath it. However, the logarithm of the switching rate is $\propto 1/\hbar$ for low temperatures, as in the case of tunneling.

We found simple explicit expressions for the switching rates both in the regime where the period-two states are the only stable states of the oscillator and where the zero-amplitude state is also stable. In the region of bistability, if the frequency detuning $\omega_F - 2\omega_0$ corresponds to the critical point, the switching activation energy scales

as $\delta F^{3/2}$ with the distance δF from the critical point along the F -axis. This scaling applies also to the switching from period-two states in the regime of tristability for arbitrary detuning (in the presence of nonlinear friction, δF should be counted off from the long-dashed bifurcation line in Fig. 6). However, generally the dependence of the activation energy on δF in the regime of bistability and the dependence on δF of the activation energy of switching from the zero-amplitude state do not display simple scaling.

In the region of tristability, depending on the field parameters, either the period-two states or the zero-amplitude state are predominantly occupied. The state occupations are close in a narrow parameter range, the behavior that reminds the first-order phase transition.

We note that parameter λ_p that characterizes the intensity of the quantum noise has also a simple spectroscopic meaning. In the absence of strong driving, the transition frequencies of the nonlinear oscillator (the distances between neighboring oscillator energy levels divided by \hbar) form a ladder. The difference between neighboring frequencies is $\lambda_p\Gamma/2$. Since Γ characterizes the level broadening, depending on λ_p one can either spectroscopically resolve transitions between different neighboring energy levels (for $\lambda_p \gg 1$) or the transitions cannot be resolved and the oscillator spectroscopically is close to a harmonic oscillator (for $\lambda_p \ll 1$). Our results refer to this second case.

ACKNOWLEDGMENTS

ZRL was supported by the RIKEN FPR program. YN was supported in part by ImPACT Program of Council for Science, Technology and Innovation (Cabinet Office, Government of Japan), the Project for Developing Innovation System of MEXT, JSPS KAKENHI (Grant No. 26220601), and National Institute of Information and Communications Technology (NICT). MID was supported in part by the U.S. Army Research Office (W911NF-12-1-0235), the National Science Foundation (DMR-1514591), and the U.S. Defense Advanced Research Agency (FA8650-13-1-7301).

-
- [1] B. Yurke, P. G. Kaminsky, R. E. Miller, E. A. Whittaker, A. D. Smith, A. H. Silver, and R. W. Simon, *Phys. Rev. Lett.* **60**, 764 (1988).
 - [2] M. A. Castellanos-Beltran, K. D. Irwin, G. C. Hilton, L. R. Vale, and K. W. Lehnert, *Nature Physics* **4**, 929 (2008).
 - [3] T. Yamamoto, K. Inomata, M. Watanabe, K. Matsuba, T. Miyazaki, W. D. Oliver, Y. Nakamura, and J. S. Tsai, *Appl. Phys. Lett.* **93**, 042510 (2008).
 - [4] C. M. Wilson, T. Duty, M. Sandberg, F. Persson, V. Shumeiko, and P. Delsing, *Phys. Rev. Lett.* **105**, 233907 (2010).
 - [5] P. Krantz, Y. Reshitnyk, W. Wustmann, J. Bylander, S. Gustavsson, W. D. Oliver, T. Duty, V. Shumeiko, and P. Delsing, *NJP* **15**, 105002 (2013).
 - [6] W. Wustmann and V. Shumeiko, *Phys. Rev. B* **87**, 184501 (2013).
 - [7] Z. Lin, K. Inomata, K. Koshino, W. Oliver, Y. Nakamura, J. Tsai, and T. Yamamoto, *Nat Commun* **5**, 4480 (2014).
 - [8] C. Eichler and A. Wallraff, *EPJ Quantum Tech.* **1**, 2 (2014).
 - [9] Z. Leghtas, S. Touzard, I. M. Pop, A. Kou, B. Vlastakis, A. Petrenko, K. M. Sliwa, A. Narla, S. Shankar,

- M. J. Hatridge, M. Reagor, L. Frunzio, R. J. Schoelkopf, M. Mirrahimi, and M. H. Devoret, *Science* **347**, 853 (2015).
- [10] L. D. Landau and E. M. Lifshitz, *Mechanics*, 3rd ed. (Elsevier, Amsterdam, 2004).
- [11] J. Guckenheimer and P. Holmes, *Nonlinear Oscillators, Dynamical Systems and Bifurcations of Vector Fields* (Springer-Verlag, New York, 1997).
- [12] M. I. Dykman, *Phys. Rev. E* **75**, 011101 (2007); in *Fluctuating Nonlinear Oscillators: from Nanomechanics to Quantum Superconducting Circuits*, edited by M. I. Dykman (OUP, Oxford, 2012) pp. 165–197.
- [13] A. Eichler, J. Moser, J. Chaste, M. Zdrojek, I. Wilson-Rae, and A. Bachtold, *Nature Nanotech.* **6**, 339 (2011).
- [14] S. Zaitsev, O. Shtempluck, E. Buks, and O. Gottlieb, *Nonlinear Dynamics*, **67**, 859 (2012).
- [15] A. Einstein and L. Hopf, *Ann.d. Phys.* **33**, 1105 (1910).
- [16] V. Weisskopf and E. Wigner, *Z. Phys.* **65**, 18 (1930).
- [17] J. Schwinger, *J. Math. Phys.* **2**, 407 (1961).
- [18] N. G. Van Kampen, *Stochastic Processes in Physics and Chemistry*, 3rd ed. (Elsevier, Amsterdam, 2007).
- [19] H. Kramers, *Physica (Utrecht)* **7**, 284 (1940).
- [20] M. Marthaler and M. I. Dykman, *Phys. Rev. A* **76**, 010102R (2007).
- [21] R. Vijay, M. H. Devoret, and I. Siddiqi, *Rev. Sci. Instr.* **80**, 111101 (2009).
- [22] M. I. Dykman and M. A. Krivoglaz, *Phys. Stat. Sol. (b)* **68**, 111 (1975).